Research Article

Journal of Chemistry Letters
journal homepage: www.jchemlett.com
ISSN (online) 2717-1892

Experimental Modelling Studies on the removal of crystal violet, methylene blue and malachite green dyes using *Theobroma cacao* (Cocoa Pod Powder).

Daniel Omeodisemi Omokpariola [a,] *

[a]*Environmental Research Units, Department of Pure and Industrial Chemistry, Nnamdi Azikiwe University, Awka, Nigeria.*

ARTICLE INFO

Article history:
Received 11 February 2021
Received in revised form 30 April 2021
Accepted 7 May 2021
Available online 7 May 2021

Keywords:
Theobroma cacao,
Modelling Studies,
Isotherms,
Kinetics,
Thermodynamics

ABSTRACT

The adsorption characteristics of basic dyes (crystal violet, CV), (methylene blue, MB) and (malachite green, MG) using *Theobroma cacao* (Cocoa pod powder), an alternative adsorbent were evaluated. Batch experiments were carried out by varying parameters such as pH, adsorbent dosage, contact time, initial dye concentration and temperature. The optimal conditions for the adsorption of CV, MB and MG on Cocoa pod powder, CCP were found have contact time (180 min), pH (4,8 and steady 6-10), temperature (333K) for an initial dye concentration of 60ppm using adsorbent dosage of 0.2g respectively. The adsorption capacity of CV, MB and MG dyes decreased with increasing CPP dosage, while there were increase with contact time and initial dye concentration. Eleven Isotherm parameters were tested with experimental data showed that CV, MB and MG dyes best fitted for Dubnin – Radushkevich, Langmuir and Freundlich isotherms. Adsorption Kinetic were modelled with Pseudo first-order, Pseudo second-order, Weber- Morris Intra-Particle diffusion, Boyd, Elovich, and Bangham. The data fitted well with Pseudo second order kinetic model compared to other kinetic models with correlation coefficient of 0.9933, 0.9981 and 0.9953 for CV, MB and MG dyes respectively. Thermodynamic parameter such as ΔG, ΔS° and ΔH° were calculated using van't hoff's and Arrhenius equations. The adsorption of CV, MB and MG increased with decreasing temperature as the process were exothermic, spontaneous and favourable in nature. Finally, the process parameter of each adsorption system is useful for developing environmental management and modelling matrices to understand best suitable system.

1. Introduction

In recent times, there is increasing awareness of water pollution from a range of pollutants, which have prompted concerted efforts towards abatement [1, 2]. Water pollution are caused by accumulation of biological, physical and chemical substances in certain concentration either by natural or synthetic source [2]. Different industrial sectors such as textile [3], paints [4], paper and pulp [5]. Pharmaceutical [6], food [7], distilleries [8], plastics [7], tannery and leather [3], cosmetics [9] and photographic and printing [7] use wide range of coloured dyes to manufacture products [10, 11], thus releasing massive amount of effluents that affects the natural aesthetics of the environment, difficult to treat and are non-biodegradable [12, 13]. Dyes effluents in small quantities can colour large water bodies, reduce sunlight penetration and photosynthesis, toxic to aquatic flora and faunas [14]. Furthermore, as these process continues, humans are entangled in the cycle by different range of exposures (ingestion, inhalation and dermal contact) that pose great risk from cancer-causing agents and death over a long period [15]. So therefore, there is a need to treat these effluents to mitigate the eventual impact to the environment as various physiochemical methodologies has been postulated to mitigate and reduce pollution impact such as ion-exchange, membrane separation, microbe, chemical and electrochemical oxidation, which

* Corresponding author. Tel.: +2348133846988; e-mail: omeodisemi@gmail.com

are not economically feasible and inefficient on large scale industries [16]. The development of finding locally available, low cost, renewable, and easy to use materials has been proposed by numerous researchers as highly efficient and selective is adsorption [17-20]. Adsorption is the most versatile and widely used procedure using adsorbent material such as alumina, silica, metal hydroxides, and activated carbon etc. has being used but are very costly on industrial scale which further lead to the incorporation of available agricultural waste produces which are left to rot from farming activities. Previous research has used agricultural wastes such as rice husk [21], coconut shells [22], saw dust [23], dead biomass [24, 25], timber waste [26] Cocoa shell [27], waste newspaper [28], rubber seed [29], groundnut shell [30] for the removal of coloured dye materials which were efficient after utilization.

Theobroma Cacao (cocoa) is an evergreen tree which is native to west Africa countries such as Nigeria, Benin, Ghana, Cote d'Ivoire etc. and other locations in Southern America that produces cocoa seeds collected from the pods are used for production of cocoa butter, chocolate, cosmetic and pharmaceutical products [31, 32]. These pods are readily available after the seeds has been used, later disposed into the environment as waste and left to rot, which aids this present research work on the utilization for batch adsorption studies for the removal of crystal violet, methylene blue and malachite green dyes respectively.

2. Materials and Methods

2.1 Preparation of Adsorbent

Theobroma Cacao (Cocoa Pod Powder, CPP) were collected from Nkwerre Local Government Area in Imo State, Nigeria. The cocoa pod were chop into small pieces, washed extensively in running water to remove dirt and particles. Thereafter sundried, ground, sieved using mesh size of 300μm and stored in an airtight container.

2.2 Preparation of Adsorbate

Crystal Violet (CV), Methylene Blue (MB) and Malachite Green (MG) are basic cationic dyes with physiochemical properties presented in **Table 1**. The respective dye solutions were prepared by dissolving 1.00g of the dye in 1L (1000ml) of distilled water. All working solution were prepared from the stock solution by further dilution.

Table 1: Physiochemical property of dyes

Property	**Crystal Violet**	**Methylene Blue**	**Malachite Green**
Chemical formula	$C_{25}H_{30}N_3Cl$	$C_{16}H_{18}ClN_3S$	$C_{23}H_{25}N_2Cl$
Chemical Structure	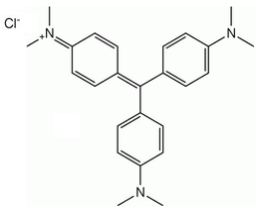	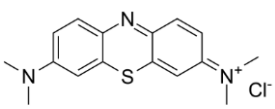	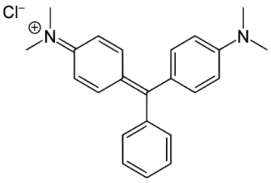
Molecular Weight	407.99 g/mol.	319.90 g/mol.	364.91 g/mol.
λ - max	590nm	668nm	617nm.
Melting Point	194°C	110°C	160°C
Colour Index	42555	52015	42000
CAS Number	548-62-9	61-73-4	569-64-2

2.3 Adsorption Studies

Experiments conducted were done using a conical flasks attached to a water bath shaker at 250 RPM running at different time intervals at room temperature (30°C) except temperature-based experiment. The concentration of dye ions before and after adsorption were determined using ultra-violet visible spectrophotometer by monitoring the absorbance at wavelength of maximum absorption for CV, MB and MG dyes.

Batch adsorption experiments were carried out by batch adsorption techniques at room temperature (30°C) with fixed adsorbent (CPP) dose of 200mg into different 250 ml conical flasks containing 30 ml of different initial concentrations (20ppm, 40ppm, 60ppm, 80ppm, 100ppm and 120ppm) of respective dye solution. The effect of adsorbent dosage were studied (20mg, 40mg, 60mg, 80mg, 100mg, 120mg, 140mg, 160mg, 180mg and 200mg) at room temperature (30°C). The effect of pH on dye removal were studied by shaking 30 ml of 60 ppm of respective dye solution concentration with 200mg adsorbent dose in conical flasks, adjusted by adding a few drops of diluted 0.1M NaOH or 0.1M HCl and measured by using a pH meter at pH of (2, 4, 6, 8, and 10). The effect of contact time and temperature were studied by shaking 30 ml of 60-ppm dye solutions concentration

with 200mg. adsorbent in a 250 ml conical flask. After definite time intervals (30 min, 60min, 90min, 120min, 150min and 180 minutes) with temperature (30, 45, 60, 75°C) on a shaker of 250 revolution per minutes (R.P.M.). After 3 hours optimum time for respective dye, samples were decanted and the filtrate were then analyzed using the ultra-violet visible spectrophotometer.

The amount of dye adsorbed onto unit weight of adsorbent, q_e (mg/g) and percentage dye removal using the equations in **Table 2**.

Table 2: Adsorption Studies

Adsorption Calculation model	Equation
Dye Uptake	$q_e = (C_o - C_e)\frac{V}{m}$
Percentage Dye Removal	$\% removal = \frac{C_o - C_e}{C_o}$

Where C_o and C_e are the initial and equilibrium adsorbate concentrations (mg/L), V is the volume of solution (L), m is the mass of the adsorbent (g).

3. Results and Discussion

After investigating the adsorption of CV, MB, and MG dyes onto CPP, the following results were attained and presented accordingly.

3.1 Effect of pH

The effect of pH on the adsorption capacity and percentage removal of CV, MB and MG dyes onto CPP were investigated at pH range of 2 to 12 as shown in **Figure 1**. It shows that pH steady increase in amount of dye being adsorbed with optimum adsorption obtained at pH: 4 and 8 for CV and MB except for MG, which show steady pH from 6 – 10. This increase can be attributed to increasing concentration of hydrogen and hydronium ions across binding site and net negative charge of adsorbent, which leads to electrostatic resistance between positive charged dyes and surface area of adsorbent is lowered resulting in an increased adsorption capacity. [27, 33].

3.2 Effect of adsorbent dosage

The adsorption capacity and percentage removal of CV, MB, MG dyes onto CPP adsorbent as presented in **Figure 2** shows a decrease from 139.6875 mg/g to 16.0405 mg/g, 113.5345mg/g to 14.4737 mg/g and 136.5517 mg/g to 16.4138 mg/g respectively with increase in adsorbent dosage from 20mg to 200mg. The optimum percentage removal were 98.8525%, 96.4919%, and 96.769%, we observed that as adsorbent dosage increased, the amount of dye adsorbed decreased due to increase in vacant adsorbent site and electrostatic interactions thus favouring adsorption. [34, 35].

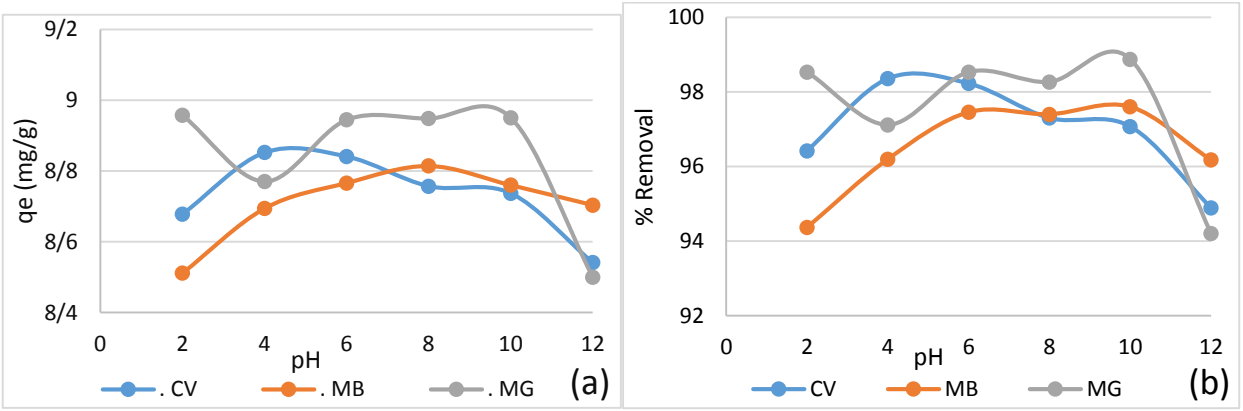

Figure 1: Effect of pH on adsorption capacity and percentage removal of CV, MB, MG dyes onto CPP

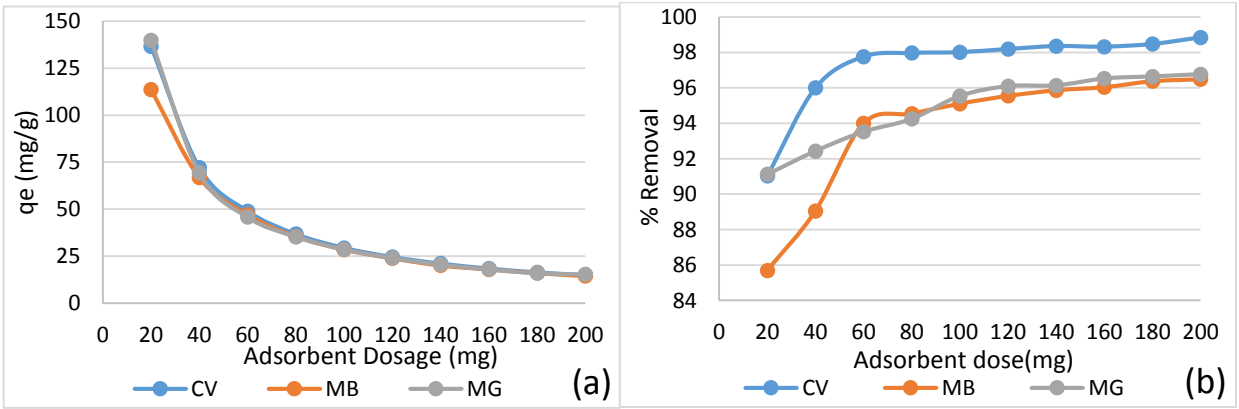

Figure 2: Effect of adsorbent dosage on adsorption capacity and percentage removal of CV, MB, MG dyes onto CPP

3.3 Effect of contact time

The effect of contact time on adsorption capacity and percentage removal of CV, MB and MG dyes using CPP presented in **Figure 3**. The results shows that dye uptake q_e, increased from 19.9297 mg/g to 24.9852 mg/g, 8.3956 mg/g to 19.7793 mg/g, and 6.3281 mg/g to 26.3843 mg/g respectively as time increased from 30 min to 120 min at initial stage, later on attained equilibrium at 180 min. The optimum percentage removal were 98.2163%, 97.5478% and 99.0863% respectively, which is due to rapid sorption at initial stage by abundance of active site on adsorbent surface and later on attained equilibrium from repulsion between adsorbate and bulk adsorbent saturation [36 – 38].

3.4 Effect of initial dye concentration

The impact of initial dye concentration on adsorption of CV, MB and MG dyes with CPP adsorbent are presented in **Figure 4**. As seen, the adsorption capacity increased steadily with initial dye concentrations at 4.1592 mg/g to 18.1367 mg/g, 2.7960 mg/g to 17.3777 mg/g and 7.0104 mg/g to 17.4688 mg/g respectively as dye concentration increased from 20 mg/l to 80mg/l equilibrium level for CV and MG dyes while MB attained equilibrium at 100mg/l. The percentage removal 98.7315%, 98.4667% and 96.5427%, which connote to the fact that the barrier to mass transfer of dye with adsorbent surface is overcome due to an increased driving force of concentration gradient with increasing initial dye concentration [33, 39, 40].

3.5 Effect of temperature

The effect of temperature on adsorption capacity and percentage removal of CV, MB and MG dyes using CPP as adsorbent presented in **Figure 5**. There were increase in adsorption capacity across dyes as temperature increased from 30ºC to 75ºC due to high mobility of ions of dyes, producing a swelling effect within the internal structure of the adsorbent [41-43].

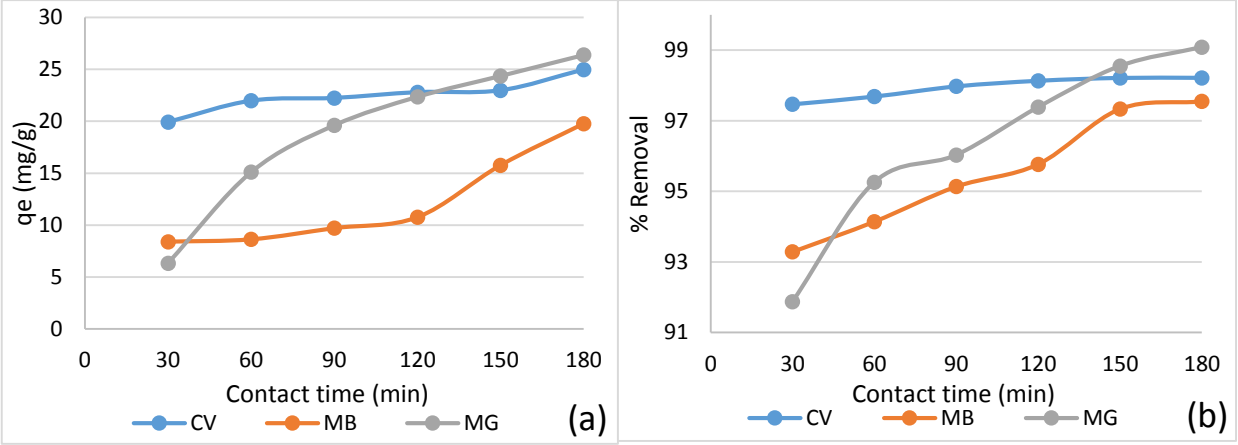

Figure 3: Effect of contact time on adsorption capacity and percentage removal of CV, MB, MG dyes onto CPP

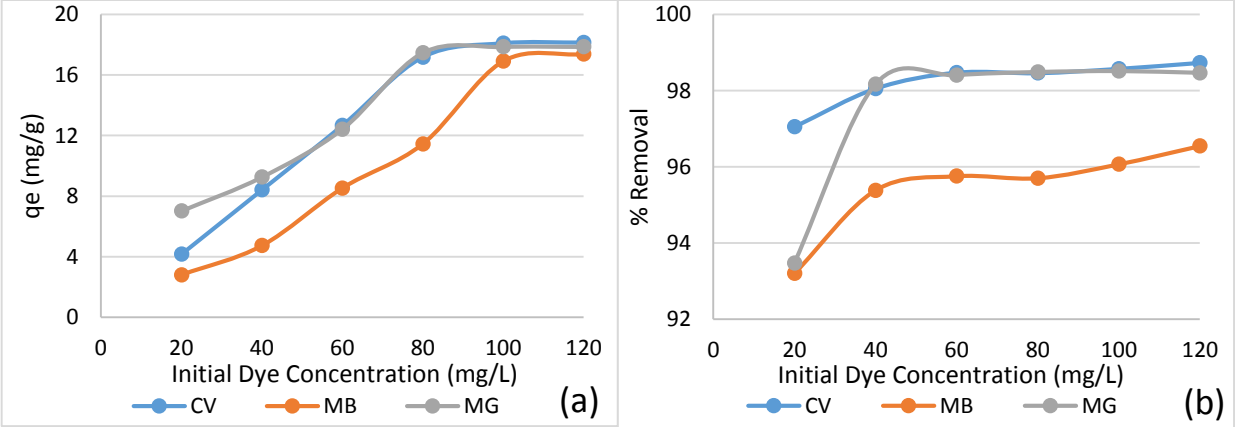

Figure 4: Effect of initial dye concentration on adsorption capacity and percentage removal of CV, MB, MG dyes onto CPP

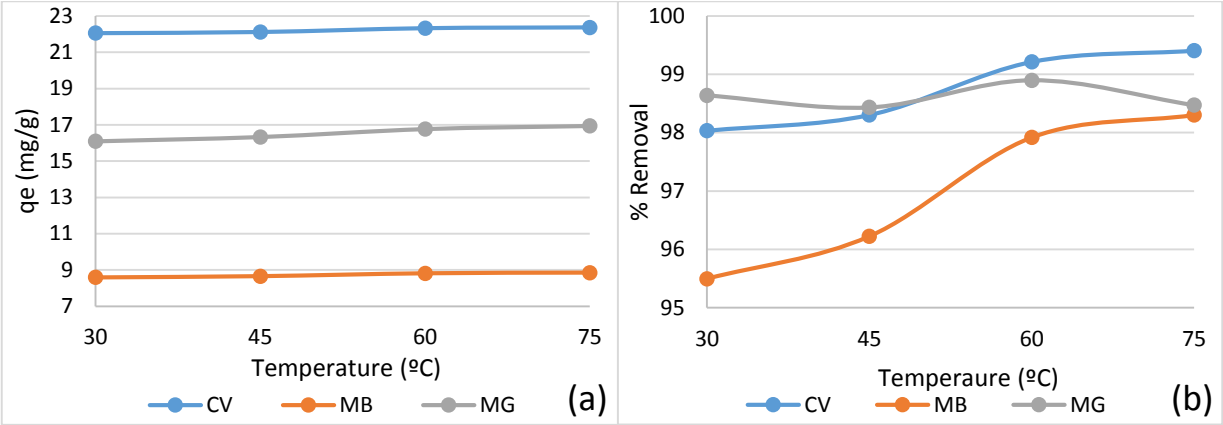

Figure 5: Effect of Temperature on adsorption capacity and percentage removal of CV, MB, MG dyes onto CPP

3.6 Adsorption Isotherm Modelling

Adsorption Isotherm describe the amount of adsorbate on the adsorbent as a function of its pressure (i.e. gas) or concentration (i.e. liquid) at constant adsorbent, pH, temperature and time. Adsorption isotherm models are mathematical tools to find most appropriate correlation for equilibrium, used to optimize adsorption experiment as used by previous studies [27, 33, 37, 39, 43 – 46].

Several Isotherm models were assessed to check which fit with respective dyes. Langmuir isotherm valuates the monolayer coverage and constant binding energy between surface and adsorbate on homogeneous surface [47, 48]. Freundlich isotherm estimates multilayer adsorption with active sites interaction on heterogeneous surfaces [49-51]. Temkin isotherm evaluates adsorbate/ adsorbent interaction on adsorption process. [52-54]. Dubnin- Radushkevich isotherm assesses both homogeneous and heterogeneous surfaces with interaction of Gaussian energy distribution that is temperature dependent [55, 56]. Halsey isotherm measure the multilayer adsorption at relatively large distance from surface [57, 58]. Harkin-Jura isotherm estimates the multilayer adsorption on adsorbent having heterogeneous surfaces [59]. Jovanovic isotherm is based on assumptions from Langmuir isotherm via mechanical contacts between adsorbent and adsorbate [60, 61]. Elovich isotherm measures the multilayer adsorption from kinetics of chemisorption of liquid onto solids [62-64]. Redlich-Peterson isotherm combines both Langmuir and Freundlich isotherms which mechanism is from a multilayer adsorption surfaces. [65-67]. Sips isotherm quantify the combination of Langmuir and Freundlich isotherms, which is used on heterogeneous surfaces [68-70]. Jossens isotherm evaluates the energy distribution of adsorbent and adsorbate interactions at heterogeneous surface [71]. The isotherm equations and its derivatives discussed are presented in **Table 3**.

Table 3: Adsorption isotherm models and its derivatives

Isotherm Model	Equation	Linear form	Plot
Langmuir 1	$q_e = \frac{q_m K_L C_e}{1 + K_L C_e}$	$\frac{C_e}{q_e} = \frac{1}{q_m K_L} + \frac{C_e}{q_m}$	$\frac{C_e}{q_e}$ vs C_e
Langmuir 2		$\frac{1}{q_e} = \frac{1}{K_L q_m}\frac{1}{C_e} + \frac{1}{q_m}$	$\frac{1}{q_e}$ vs $\frac{1}{C_e}$
Freundlich	$q_e = K_F C_e^{1/n}$	$\log q_e = \log K_F + {}^1/_n \log C_e$	$\log q_e$ vs $\log C_e$
Temkin	$q_e = \beta \ln(K_T C_e)$, where, $\beta = \frac{RT}{b}$	$q_e = \left(\frac{RT}{b}\right)\ln K_T + \left(\frac{RT}{b}\right)\ln C_e$	q_e vs $\ln C_e$
Dubnin-Radushkevich	$q_e = q_m \exp(-K_{DR}\varepsilon^2)$ where, $\varepsilon = RT\ln\left(1 + \frac{1}{C_e}\right)$	$\ln q_e = \ln q_m - K_{DR}\varepsilon^2$ $E = \frac{1}{\sqrt{2K_{DR}}}$	$\ln q_e$ vs ε^2
Halsey	$q_e = \exp(K_H C_e)^{1/n_H}$	$\ln q_e = \left(\frac{1}{n_H}\right)\ln K_H - \left(\frac{1}{n_H}\right)\ln C_e$	$\ln q_e$ vs $\ln C_e$
Harkin-Jura	$\frac{1}{q_e^2} = \frac{B}{A} + \left(\frac{1}{A}\right)\log C_e$	$\frac{1}{q_e^2} = \frac{B}{A} + \left(\frac{1}{A}\right)\log C_e$	$\frac{1}{q_e^2}$ vs $\log C_e$
Jovanovic	$q_e = q_m \exp(K_J C_e)$	$\ln q_e = \ln q_m - K_J C_e$	$\ln q_e$ vs $\ln C_e$

Elovich	$\ln\left(\frac{q_e}{C_e}\right) = \ln(K_E q_m) - \frac{q_e}{q_m}$	$\ln\left(\frac{q_e}{C_e}\right) = \ln(K_E q_m) - \frac{q_e}{q_m}$	$\ln\left(\frac{q_e}{C_e}\right)$ vs q_e
Redlich-Peterson	$q_e = \frac{AC_e}{1 + BC_e{}^{\beta}}$	$\ln\left(\frac{C_e}{q_e}\right) = \beta \ln C_e - \ln(A)$ where, $A/B = K_F$	$\ln\left(\frac{C_e}{q_e}\right)$ vs $\ln C_e$
Sips	$q_e = \frac{K_s C_e^{\beta_s}}{1 + a_s C_e^{\beta_s}}$	$\beta_s \ln C_e = \ln\left(\frac{K_s}{q_e}\right) + \ln a_s$	$\ln C_e$ vs $\ln\left(\frac{1}{q_e}\right)$
Jossens	$C_e = \frac{q_e}{H} \exp(F q_e{}^{P})$	$\ln\left(\frac{C_e}{q_e}\right) = -\ln(H) + (F q_e{}^{P})$	$\ln\left(\frac{C_e}{q_e}\right)$ vs q_e

Where q_e = amount of adsorbate adsorbed at equilibrium (mg/g), Ce = equilibrium concentration of adsorbate (mg/l), q_m = maximum adsorption capacity. , K_L= Langmuir constant related to the affinity of the binding sites and energy of adsorption (L/mg), K_F = Freundlich isotherm, which is adsorption capacity (L/mg), 1/n = is adsorption capacity, K_T = Temkin constant (L/g), β = constant related to heat of adsorption, b = Temkin isotherm constant related to heat of adsorption (J/mol), R = universal gas constant (8.314J/mol./K). T = Temperature at 303K, K_{DR} = Dubnin – Radushkevich constant due to free energy of adsorption (mol^2/J^2), ε = Polanyi potential (J/mol.), which is related to the equilibrium constant (C_e), E = free energy of adsorption (J/mol.), K_H and n_H are Halsey isotherm constant, B and A are Harkin – Jura isotherm constant, K_J = Jovanovic constant, K_E = Elovich constant. A, B, β = are Redlich – Peterson constant, K_S and a_s = Sips isotherm constant (L/g), β_s is Sips isotherm model constant, H, P and F = are Jossens isotherm constant.

Table 4 and Figures 6-8 shows the isotherm models assessed conducted on CV, MB and MG dyes onto CPP adsorbent its applicability in environmental assessment and modelling studies. In decreasing order for CV dye, the correlation coefficient were Dubnin-Radushkevich > Temkin > Langmuir 2 > Freundlich > Halsey > Sips > Langmuir 1 > Elovich > Jovanovic > Redlich-Peterson > Harkin-Jura > Jossen. For MB dye, Langmuir 2> Jovanovic > Elovich > Jossen > Freundlich > Halsey > Sips > Dubnin-Radushkevich > Harkin-Jura > Langmuir 1 > Temkin > Redlich-Peterson. For MG dye, Freundlich > Halsey > Sips > Temkin > Jovanovic > Dubnin-Radushkevich > Langmuir2 > Elovich > Harkin-Jura > Redlich-Peterson > Langmuir-1 > Jossen. As shown in the table, Freundlich, Halsey and Sips isotherms were predominant in that they had similar coefficient of correlation (R^2) and plot equation for all dyes, thus affirm any of them can be utilized concurrently.

We can therefore state that crystal violet dye (CV) were best fitted at Dubnin-Radushkevich and least fitted with Jossens. Maximum adsorption at equilibrium, q_m were achieved at 19.32 mg/g compared to Langmuir-2 with q_m at 54.95 mg/g; which shows that the process can go through physiosorption than chemisorption process due to the Energy value of each dye 1.58KJ/mol, 0.71KJ/mol and 1.12KJ/mol respectively [72]. Methylene blue dye (MB) were fitted to Langmuir 2 isotherm due to homogenous dispersal and formation of monolayer coverage between energetic sites on adsorbent surface [73]. Malachite green dye (MG) were best fitted to Freundlich isotherm indicating the CPP adsorbent surfaces were heterogeneous and went through chemisorption [74].

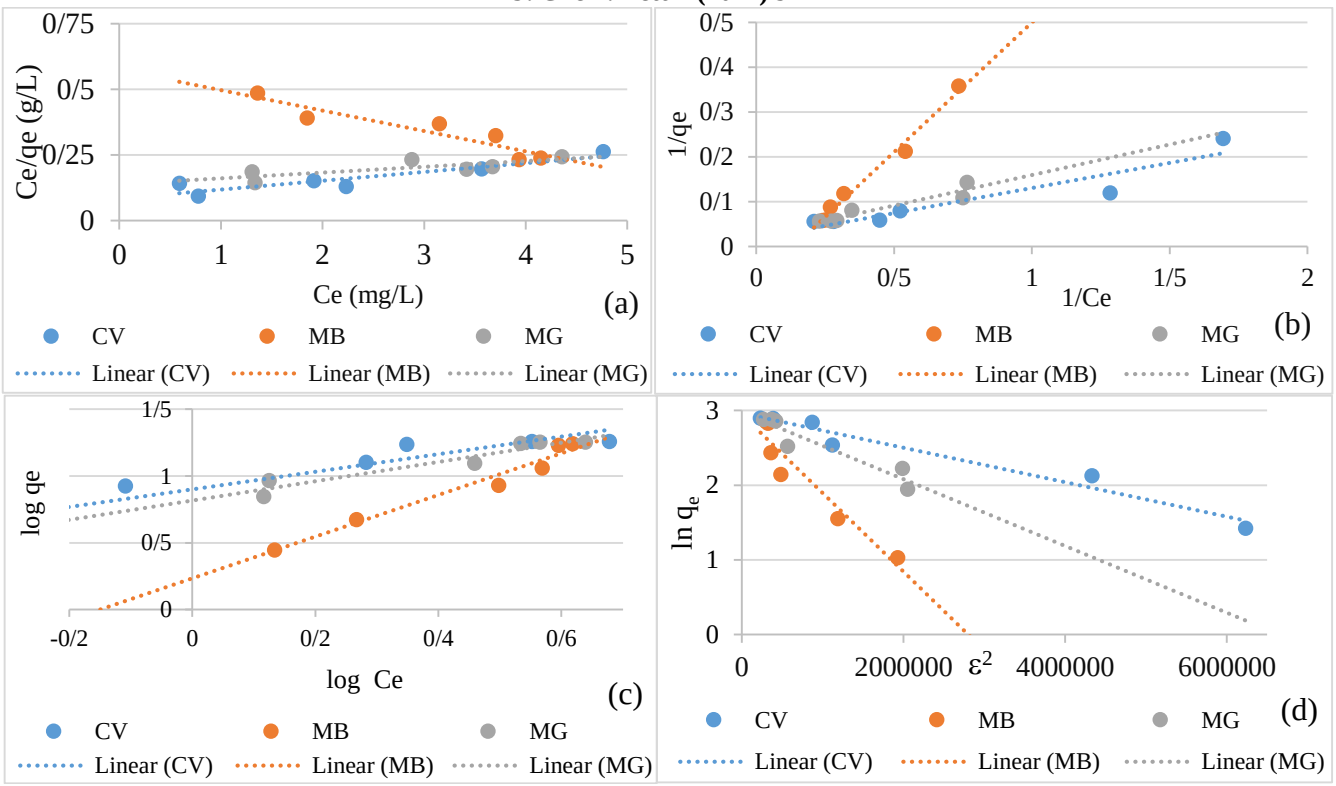

Figure 6: Adsorption isotherm plots (a) Langmuir isotherm- 1; (b) Langmuir Isotherm – 2; (c) Freunlich isotherm; (d): Dubnin-Radushkevich isotherm.

Table 4: Isotherm parameters for adsorption of CV, MB and MG dyes onto CPP

Isotherm Model	Isotherm Parameter	Crystal Violet (CV)	Methylene Blue (MB)	Malachite Green (MG)
Langmuir (I), L1	q_m (mg/g)	29.7619	12.8535	45.4545
	K_L (L/mg)	0.3948	0.1352	0.1584
	R^2	0.8309	0.8665	0.6144
	Equation	y=0.0336x+0.0851	y=-0.0778x+0.5755	y=0.022x+0.1389
Langmuir (II), L2	q_m (mg/g)	54.9450	12.6422	43.1034
	K_L (L/mg)	0.1624	0.1367	0.1707
	R^2	0.8770	0.9858	0.8922
	Equation	y=0.1121x+0.0182	y=0.5787x-0.0791	y=0.1359x+0.0232
Freundlich, F	K_F (L/mg)	7.9287	1.7136	6.5433
	n	33.165	7.3052	1.0003
	R^2	0.8599	0.9659	0.9163
	Equation	y=0.6576x+0.8992	y=1.5579x+0.2339	y=0.7211x+0.8158
Dubnin-Radushkevich, DR	q_m (mg/g)	19.3192	19.5857	18.9974
	K_{DR} (mol^2/J)	2.0E-07	1.0E-06	4.0E-07
	E (J/mol)	1581.1388	707.1068	1118.0340
	R^2	0.9580	0.9115	0.8935
	Equation	y=-2e-07x+2.9611	y=-1e-06x+2.9443	y=-4e-07x+2.9748
Temkin, T	K_T (L/g)	0.1093	0.4461	0.1811
	β	6.7652	12.1920	8.6868
	b	372.3677	206.6225	289.9965
	R^2	0.9228	0.8459	0.9105
	Equation	y=6.7652x+9.1515	y=12.192x-2.2417	y=8.6868x+5.5224
Halsey, H	K_H (L/mg)	23.3072	1.4130	13.5326
	n	1.5207	0.6419	1.3868

	R^2	0.8599	0.9659	0.9163
	Equation	y=0.6576x+2.0706	y=1.5579x+0.5386	y=0.7211x+1.8785
Harkin-Jura, HJ	B (L/mg)	0.5635	0.5935	0.6982
	A (mg/g)	21.1864	4.3898	36.3636
	R^2	0.6146	0.8678	0.8340
	Equation	y=-0.0472x+0.0266	y=-0.2278x+0.1352	y=-0.0275x+0.0192
Jovanovic, JC	q_m (mg/g)	1.7752	0.2635	1.7082
	K_J (L/mg)	0.2946	0.6208	0.2989
	R^2	0.6608	0.9764	0.9006
	Equation	y=0.2946x+1.7752	y=0.6208x+0.2635	y=0.2989x+1.7082
Elovich, E	q_m (mg/g)	30.9598	21.3675	23.8663
	K_e (L/mg)	1.0720	1.0230	1.0998
	R^2	0.8126	0.9685	0.8458
	Equation	y=-0.0323x+2.1529	y=0.0468x+0.6308	y=-0.0419x+2.2713
Redlich-Peterson , RP	A (L/g)	2.0706	0.5386	1.8785
	B (L/mg)	0.2611	0.3143	0.2871
	β	0.3424	0.5579	0.2789
	R^2	0.6246	0.7844	0.6209
	Equation	y=0.3424x-2.0706	y=-0.5579x-0.5386	y=0.2789x-1.8785
Sips, S	K_s (L/g)	0.5181	0.2106	0.4862
	a_s (L/g)	0.1261	0.5836	0.1528
	R^2	0.8599	0.9659	0.9163
	Equation	y=-0.6576x-2.0706	y=-1.5579x-0.5386	y=-0.7211x-1.8785
Jossens, JS	H	10.6196	1.8791	6.8613
	F	0.0376	0.0468	0.0226
	R^2	0.3728	0.9685	0.3374
	Equation	y=0.0376x-2.3627	y=-0.0468x-0.6308	y=0.0226x-1.9259

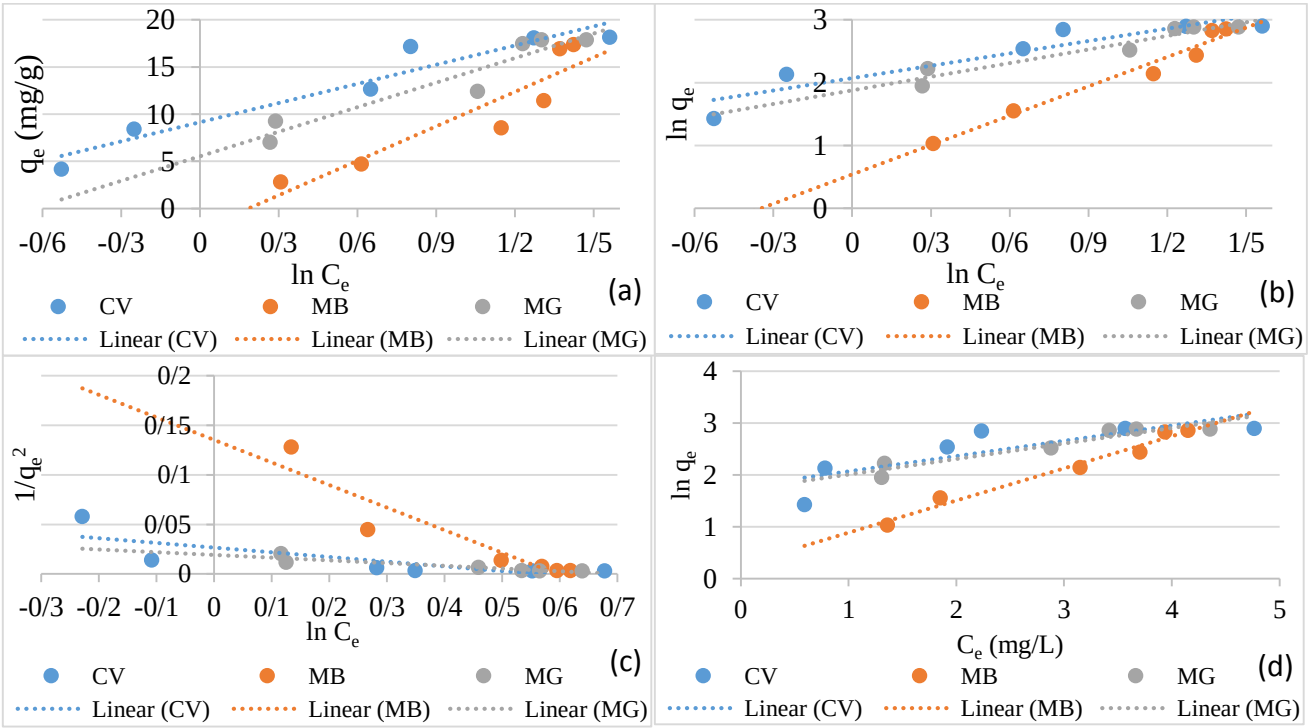

Figure 7: Adsorption isotherm plots (a) Temkin isotherm; (b) Halsey isotherm; (c) Harkin-Jura isotherm; (d): Jovanoic isotherm.

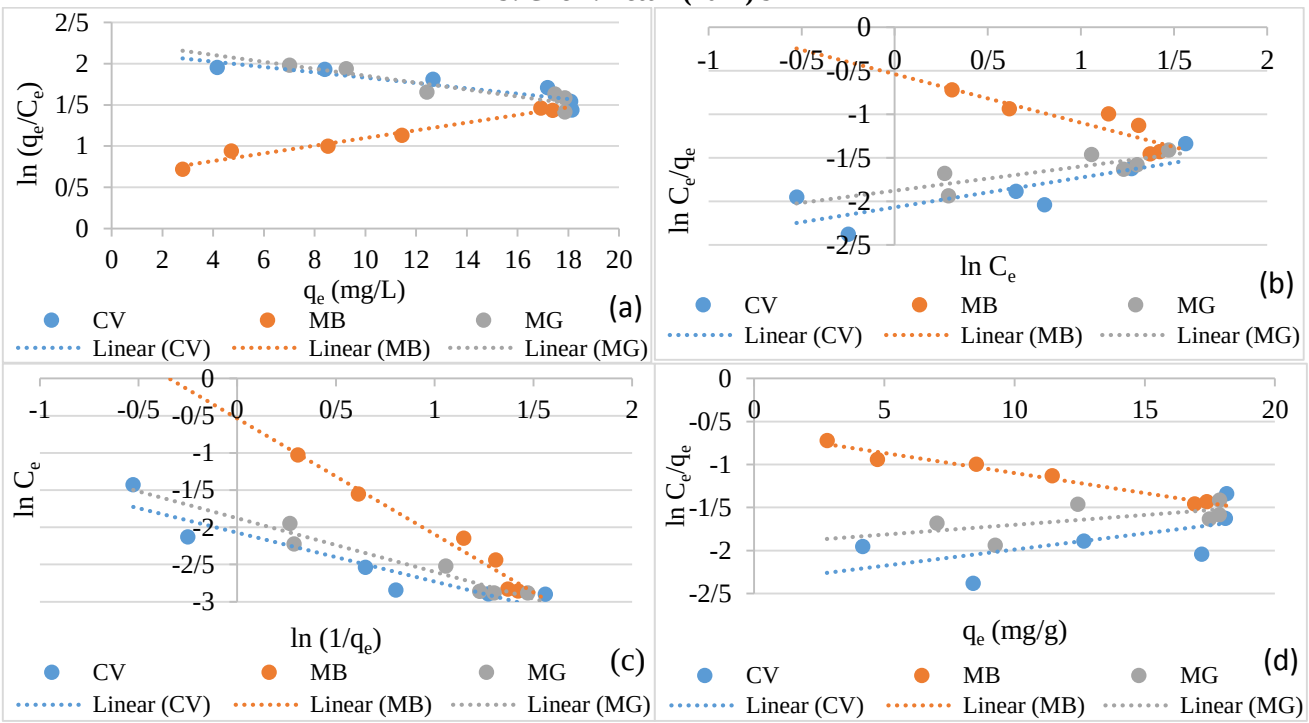

Figure 8: Adsorption isotherm plots (a) Elovich isotherm; (b) Redlich-Peterson isotherm; (c) Sips isotherm; (d): Jossens isotherm.

3.6 Adsorption Kinetic Modelling

Adsorption kinetics describes the rate of retention of solute from aqueous phase to solid phase at given adsorbent dose, temperature and pH. Different kinetic models were utilized to get best fit for respective dyes which includes Pseudo first-order, Pseudo second-order, Weber- Morris Intra-Particle diffusion, Boyd, Elovich, Bangham.

Pseudo first-order model investigates the relationship between the rate of occupied adsorbent site and unoccupied sites [75]. Pseudo second-order model describes the adsorption capacity of adsorbent based on time [76 – 78]. Weber – Morris (intra-particle diffusion) model examines the rate limiting step during adsorption process [79, 80], Boyd model analyses the actual slow step involved in the adsorption process [81-83]. Elovich model evaluates adsorption onto heterogeneous surfaces [84, 85]. Bangham model evaluates the dominance of pore diffusion in adsorption process [86, 87]. The adsorption kinetic model equations are presented in **Table 5** to plot respective graphs in **Figure 9-11**.

Table 5: Adsorption Kinetic models and its derivatives

Kinetic Model	**Equation**	**Linear form**	**Plot**
Pseudo First Order	$q_t = q_e(1 - exp^{-k_1 t})$	$\ln(q_e - q_t) = lnq_e - k_1 t$	$\ln(q_e - q_t)\ vs\ t$
Pseudo Second Order I	$q_t = \frac{k_2 {q_e}^2 t}{1 + K_2 q_e t}$	$\frac{t}{q_t} = \left(\frac{1}{k_2 {q_e}^2}\right) + \frac{1}{q_e} t$	$\frac{t}{q_t}\ vs\ t$
Pseudo Second Order II		$\frac{1}{q_t} = \left(\frac{1}{k_2 {q_e}^2}\right)\left(\frac{1}{t}\right) + \frac{1}{q_e}$	$\frac{1}{q_t} vs\ \frac{1}{t}$
Weber – Morris (Intra-Particle Diffusion)	$q_t = k_{IP} \times t^{1/2}) + C_i$		$q_t\ vs\ t^{1/2}$
Boyd	$F = 1 - \frac{6}{\pi^2}\sum_1^\infty \left(\frac{1}{n^2}\right) \exp(-n^2 B_t)$ $B_t = -0.497 - \ln(1 - F).\ where, F = \frac{q_t}{q_\infty}$		$B_t vs\ t$
Elovich	$\frac{dq_t}{dt} = \propto exp^{-\propto q_t}$	$q_t = \frac{1}{\beta}\ln \alpha\beta + \frac{1}{\beta}\ln t$	$q_t\ vs\ ln\ t$

Bangham	$log.log\left(\frac{C_o}{C_o - q_t M}\right) = log\left(\frac{K_o}{2.303V}\right) + \propto log\, t$	$log.log\left(\frac{C_o}{C_o - q_t M}\right)\ vs \log t$

Where q_t and q_e = are the amount of dye adsorbed (mg/g) at time t and at equilibrium, k_1 = Rate constant of the pseudo-first order (min^{-1}), t = time (min), k_2 = Rate constant of the pseudo-second order (g/mg/min), k_{IP}= Intra-particle rate constant ($mg/g/min^{1/2}$), C = Intercept of plot. F = Fraction of solute adsorbed at time t (q_t) at infinite time (q_∞), B_t is a function of F, α = initial rate of adsorption (mg/g/min), β = extent of surface coverage (g/mg), M = mass of adsorbent used (g), V = volume of dye solution (mL), K_o and α are constant.

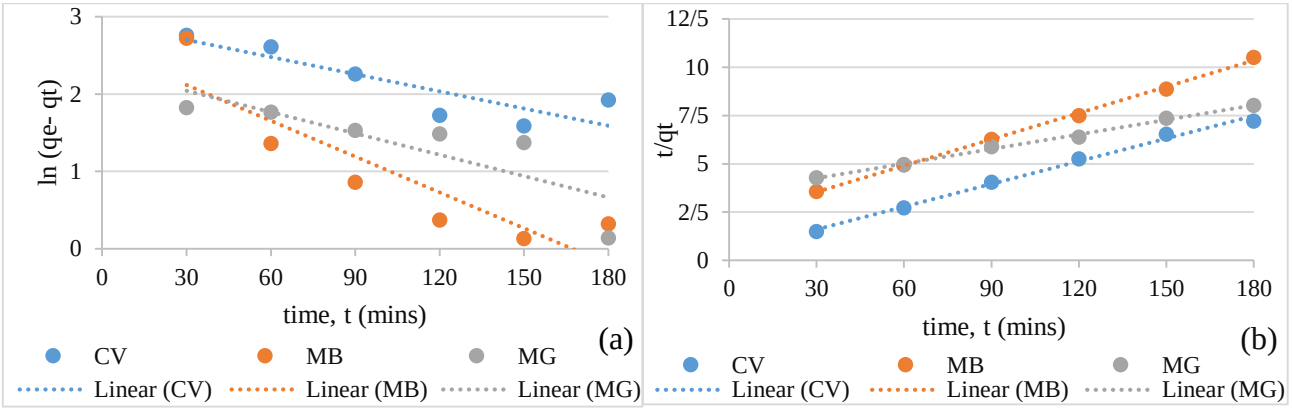

Figure 9: Adsorption kinetic plots (a) Pseudo first order kinetic model; (b) Pseudo-second order-1 kinetic model

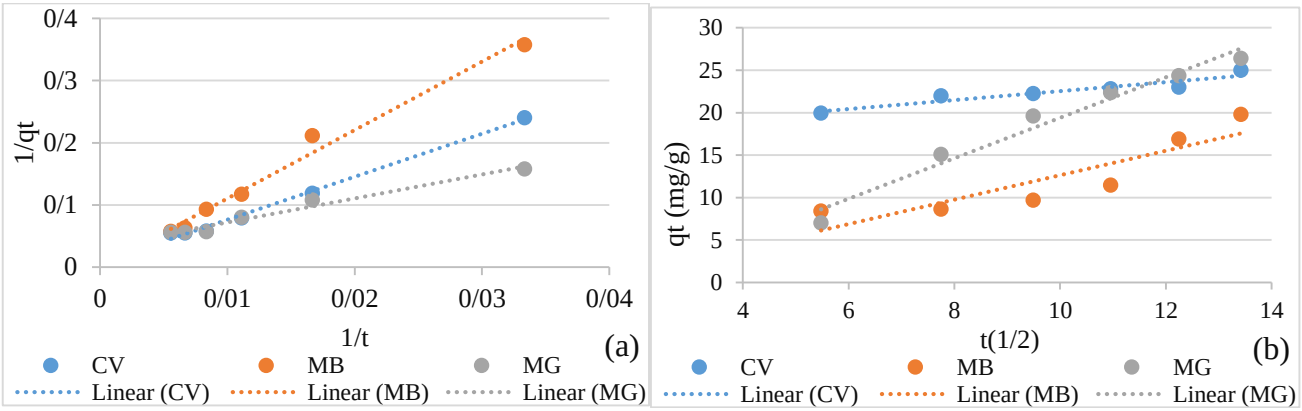

Figure 10: Adsorption kinetic plots (a) Pseudo-second order-2 kinetic model; (b) Weber–Morris (Intra-particle diffusion) kinetic model.

Table 6 shows the adsorption kinetic models studied for the adsorption of CV, MB and MG dyes with CPP as adsorbent. In decreasing other, the correlation coefficient of CV dye implies that Pseudo second order 1 > Pseudo second order 2 > Elovich > Bangham > Weber Morris > Boyd > Pseudo first order. For MB dye, Pseudo second order 2 > Pseudo second order 1 > Elovich > Bangham > Boyd > Weber Morris >Pseudo first order. For MG dye, Pseudo second order 1 > Boyd > Pseudo second order 2 > Weber Morris > Elovich > Bangham > Pseudo first order. So therefore, CV, MB and MG shows that Pseudo second order were greater than other kinetic models assessed, which confirms that the process is the best fit kinetic models and went through chemical adsorption [74, 76]. This implies that the adsorption process is dependent on rate phase via electron exchange between adsorbent and adsorbate [87].

Table 6: Kinetics Parameters for adsorption of CV, MB and MG onto CPP

Kinetic Model	Kinetic Parameter	Crystal Violet (CV)	Methylene Blue (MB)	Malachite Green (MG)
Pseudo-First Order	k_1 (1/min)	0.0074	0.0092	0.0154
	q_e (mg/g)	18.5543	13.1853	10.1381
	R^2	0.7566	0.7925	0.6944
	Equation	y=-0.0074x+2.9707	y=-0.0154x+25791	y=-0.0092x+2.3163
Pseudo-Second Order (1)	k_2 (g/mg min)	0.0035	9.3878E-04	1.8149E-04
	q_e (mg/g)	25.5754	22.0751	39.6825
	h	285.7143	1065.2123	5509.9454
	R^2	0.9933	0.9981	0.9953
	Equation	y=0.0391x+0.4356	y=0.0453x+2.1859	y=0.0252x+3.4991
Pseudo-Second Order (2)	k_2 (g/mg min)	7.0852E-06	5.8066E-10	2.9099E-04
	q_e (mg/g)	142.8571	12,500	29.8507
	R^2	0.9930	0.9848	0.9733
	Equation	y=6.9158x+0.007	y=11.022x+8E-05	y=3.8566x+0.0335
Weber-Morris (Intra-Particle Diffusion)	k_i (mg/g $min^{1/2}$)	0.5254	1.4414	2.3823
	C	17.292	1.7765	4.4183
	R^2	0.8905	0.7954	0.9694
	Equation	y=0.5254x+17.292	y=1.4414x-1.7765	y=2.3823x-4.4183
Boyd	m(x) (min)	0.0086	0.0190	0.0047
	C	0.4386	0.5047	0.1055
	R^2	0.8250	0.8888	0.9740
	Equation	y=0.0086x-0.4386	y=0.019x-0.5047	y=0.0047x+0.1055
Elovich	1/β	8.6275	8.3499	7.2872
	lnαβ	2.9787	3.3011	2.6408
	R^2	0.9663	0.8994	0.9365
	Equation	y=8.6275x-25.699	y=8.3499x-27.564	y=7.2872x-19.244
Bangham	α	-0.0019	-0.0019	-0.0016
	K_o	277.9811	277.5333	278.0451
	R^2	0.9657	0.8971	0.9355
	Equation	y=-0.0019x+0.6046	y=-0.0019x+0.6047	y=-0.0016x+0.6039

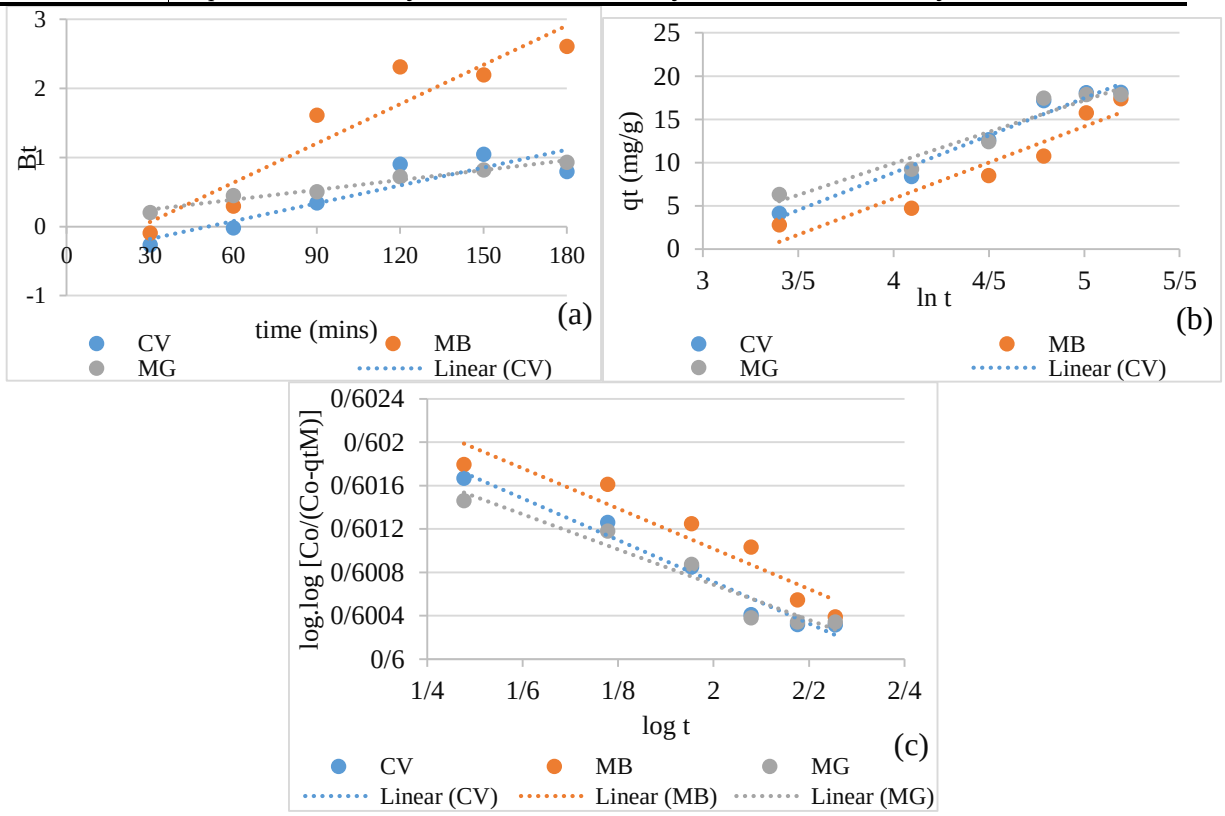

Figure 10: Adsorption kinetic plots (a) Boyd kinetic model; (b) Elovich kinetic model; (c) Bangham kinetic model

3.6 Adsorption Thermodynamics Modelling

Adsorption thermodynamics is used to determine the spontaneity or non-spontaneity of adsorption process using temperature at constant time, adsorbent dose, pH and concentration. The thermodynamic parameters such as Gibbs free energy change (ΔG) were calculated and evaluated using Van't Hoff's [70, 88].and Arrhenius [72] equations as represented in **Table 7** and graphs were plotted as shown in **Figure 11**.

Table 7: Adsorption Thermodynamics and its derivatives

Adsorption Calculation model	Equation	Plot
Gibbs free energy change	$\Delta G = \Delta H^{\circ} - \Delta S^{\circ};$ $\Delta G = -RT\ln K_c$ where, $K_C = \frac{q_e}{C_e}$	
Van't Hoff's Equation	$\ln K_c = \frac{\Delta S^{\circ}}{R} - \frac{\Delta H^{\circ}}{RT}$	$\ln K_c$ vs $1/T$
Arrhenius equation	$\ln K_c = \ln A - \frac{E_a}{RT}$	$\ln K_c$ vs $1/T$

Where ΔG = Gibb's free energy, ΔS° and ΔH° = change in entropy and enthalpy, R = universal gas constant (8.314J/mol./K). T = Temperature (K), K_C = equilibrium rate constant, A = Arrhenius constant (J/mol/K), Ea = activation energy (KJ/mol).

Table 8 shows thermodynamic parameters calculated from the plots for CV, MB and MG onto CPP as adsorbent. The negative values from change in enthalpy indicates that adsorption process were exothermic in nature as change in entropy, ΔS were positive which suggest that adsorption went with increasing randomness at absorbent/adsorbate surfaces. Gibbs' free energy were negative across different temperatures as ΔG decreased as temperature increased, thus implies that adsorption will require lower temperature to be efficient and have low energy barrier [88, 89].

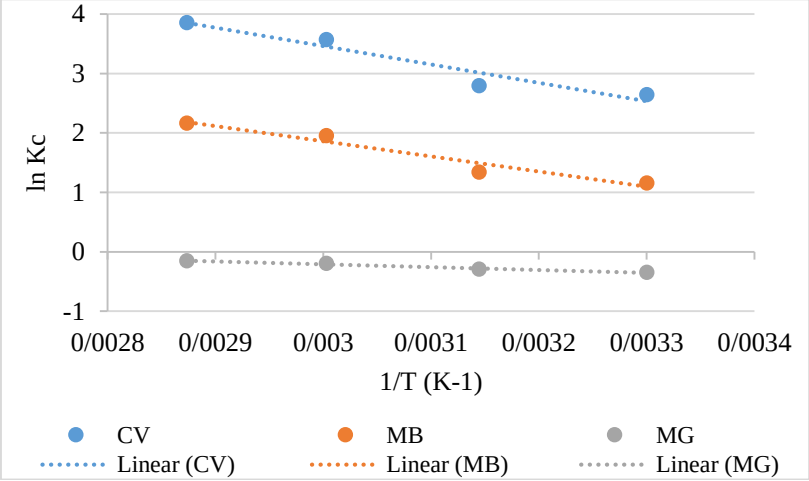

Figure 11: Adsorption thermodynamic plots: Van't Hoff's and Arrhenius thermodynamic model

Table 8: Thermodynamics parameter for CV, MB and MG adsorption unto CPP

Models	Thermodynamic Parameter	Temperature (K)	Crystal Violet (CV)	Methylene Blue (MB)	Malachite Green (MG)
Van't Hoff's	ΔH (KJ/mol)		–3.0880	–2.5464	–0.4793
	ΔS (J/mol/K)		12.7260	9.4972	1.2284
	ΔG (KJ/mol)	303K	–7.3769	–2.9139	0.1514
		318K	–8.1399	–3.5436	0.0199
		333K	–10.6781	–5.4096	–0.2570
		348K	–11.9772	–6.2560	–0.3868
	R^2		0.9279	0.9462	0.9755

	Equation	y=-3088x+12.726	y=-2546x+9.4972	y=-479.27x+1.2284
Arrhenius	E_a (KJ/mol)	25.6736	21.1708	3.9847
	A ($\times 10^{-3}$)	336.3811	13.3224	0.0034

4. Conclusion

Experimental and modelling studies has been carried out for the removal of crystal violet (CV), methylene blue (MB) and malachite green (MG) dyes using cocoa pod powder (CCP) were reported. Adsorption parameters such as pH, adsorbent dosage, contact time, initial dye concentration and temperature were optimized. The adsorption capacity of all dyes decreased with increasing dosage, as dye removal increased with increasing temperature, initial dye concentration, contact time and pH level of 4, 8 and 6-10 for CV, MB and MG dyes. Eleven isotherm models were assessed to infer which is best suited for experimental studies. Dubnin – Radushkevich were compactible with CV dye, Langmuir fitted for MB dye and Freundlich fitted for MG dye. Kinetic studies assessed showed that Pseudo-second order were appropriate for all dyes. Thermodynamic parameters showed negative Gibb's free energy and enthalpy with positive entropy thus confirms the process is exothermic, spontaneous and favourable in nature and that the process requires lower temperature for adsorption to take place efficiently. So therefore, *Theobroma cacao* (cocoa pod powder) is an effective, cheap alternative and available adsorbent useful for the removal of CV, MB and MG dyes in effluent treatment plant processes, as the adsorbent (CCP) utilized after adsorption can further be degraded by microbes for biogas production or non-toxic byproducts that keeps the environment clean and green.

Acknowledgements

The author acknowledge the laboratory analysts of Department of Chemistry, Federal Univerisity of Technology, Owerri, Nigeria and Department of Chemistry, Imo State University, Owerri, Nigeria for supporting this research work.

References

[1] O. K. Adeyemo. Consequences of pollution and degradation of Nigerian aquatic environment on fisheries resources. *The Environmentalist*, 23(4) (2003) 297-306.

[2] O.B. Adedeji and V.E. Adetunji. Aquatic Pollution in Nigeria: The Way Forward. *Advances in Environmental Biology*, 5(8) (2011) 2024-2032.

[3] S. Mani, P. Chowdhary and R. N. Bharagava. Textile wastewater dyes: toxicity profile and treatment approaches. *Emerging Eco-friendly Approaches Waste Manag.*, (2019) 219-244

[4] M Chandhru, S Kutti Rani and N Vasimalai. Reductive degradation of toxic six dyes in industrial wastewater using diaminobenzoic acid capped silver nanoparticles. *J. Environ. Chem. Eng.* 8 (5) 2020 104225

[5] M. Ismail, K. Akhtar, M.I. Khan, T. Kamal, M.A Khan, A. M Asiri, J. Seo and S.B Khan. Pollution, toxicity and carcinogenicity of organic dyes and their catalytic bio-remediation. *Curr. Pharma. Design.* 25 (34) (2019) 3645-3663.

[6] A. Gičević, L. Hindija and A. Karačić. Toxicity of azo dyes in pharmaceutical industry. *Int. Conf. Med. Biolog. Eng.*, (2019) 581-587.

[7] J.H. Franco, B. F. Da-Silva, E.F.G. Dias, A.A De-Castro, T.C. Ramalho and M.V.B Zanoni Influence of auxochrome group in disperse dyes bearing azo groups as chromophore center in the biotransformation and molecular docking prediction by reductase enzyme. *Ecotoxicol. Environ. Safety*. 160 (2018) 114-126.

[8] P. Chowdhary, A. Yadav, G. Kaithwas and R.N. Bharagava. Distillery wastewater: a major source of environmental pollution and its biological treatment for environmental safety. *Green Technol. Environ. Sustain.*, (2017) 409-435.

[9] D. Rawat, |R.S. Sharma, S. Karmakar, L.S. Arora and V. Mishra. Ecotoxic potential of a presumably non-toxic azo dye. *Ecotoxic. Environ. Safety*, 148 (2018) 528-537

[10] K. Binod and K. Upendra Removal of malachite green and crystal violet dyes from aqueous solutions with biomaterials. *Glob. J. Res. Eng.*, 14(4) (2014) 249-255.

[11] W. Zongping, X. Miaomiao, H. Kai, I. Zizheng. Textile dyeing wastewater treatment. In: Advances in treating textile effluent, Prof. Hauser P. (Ed.), (2011). ISBN: 978-953-307-704-8 InTech.

[12] S. Haque, H. Yasmin and M.Rahman. Environmental Pollution in Bangladesh. *Organization Eco. J.* (2002). 38-47.

[13] O.B. Adedeji and V.E. Adetunji. Aquatic Pollution in Nigeria: The Way Forward. *Adv. Environ. Bio.* 5(8) (2011) 2024-2032.

[14] T.E. Seow, C.K. Lim, M.H.B. Norb, M.F.M. Mubarak, C.Y. Lam, A.Yahya, and Z. Ibrahim Review on Wastewater Treatment Technologies. *Int. J. Appl. Environ. Sci.* 11(1) (2016) 111-126.

[15] P.L. Williams, R.C. James and S.M. Roberts. Principles of Toxicology Environmental and Industrial Applications. 2nd Ed. Wiley-Interscience Publishers. (2014). ISBN 0-471-29321-0.

[16] B.H. Hammed, R.R. Krishni, and S.A. Sata, (2009). A novel agricultural waste adsorbent for the removal of cationic dye from aqueous solution. *J. Hazard. Mater.* 162(1), 305-311. https://doi.org/10.1016/j.jhazmat.2008.05.036

[17] A. Asfaram, M.R. Fathi, S. Khodadoust, M. Naraki. Removal of Direct Red 12B by garlic peel as a cheap adsorbent: kinetics, thermodynamic and equilibrium isotherms study of removal. *Spectrochimica Acta Part A: Mol. Biomolec. Spec.*, (2014) 415-421.

[18] S. Sharma and A. Kaur. Various methods for removal of dyes from industrial effluents: A review. *Indian J. Sci. Technol.* 11 (2018) 1-21.

[19] A. Gürses, K. Güneş and E. Şahin Removal of dyes and pigments from industrial effluents. *Green Chem. Water Remed: Res. App.*, (2021) 135-187.

[20] M. Sardar, M. Manna, M. Maharana and S. Sen Remediation of dyes from industrial wastewater using low-cost adsorbents. In: Green Adsorbents to Remove Metals, Dyes and Boron from Polluted Water, Springer. (2017) 377-403.

[21] Suman Mor, Kalzang Chhoden, Khaiwal Ravindra. Application of agro-waste rice husk ash for the removal of phosphate from the wastewater. *J. Cleaner Prod.*, 129 (2016) 673-680.

[22] Y.C. Wong, M.S.R. Senan and N.A. Atiqah. Removal of methylene blue and malachite green dye using different form of coconut fibre as absorbent. *J Basic Appl. Sci.* 9 (2013) 172-177.

[23] S. Shamohammadi. Study of Kinetics of Copper in Aqueous Solution by Sawdust Adsorbent. *J. Water – Wastewater*, 23 (2) (2012) 127-133.

[24] W. Lang, C. Dejma, S. Sirisansaneeyakul and N. Sakairi. Biosorption of nonylphenol on dead biomass of *Rhizopus arrhizus* encapsulated in chitosan beads. *Biores. Technol.*, 100 (23), (2009) 5616-5623.

[25] M. Tavana, H. Pahlavanzadeh and M. J. Zarei The novel usage of dead biomass of green algae of *Schizomeris leibleinii* for biosorption of copper (II) from aqueous solutions: Equilibrium, kinetics and thermodynamics. *J. Environ. Chem. Eng.*, 8 (5), (2020) 104272

[26] Y.C. Uma and P. Sharma. Removal of Malachite Green from Aqueous Solutions by Adsorption on to Timber Waste. *Int. J. Environ. Eng. Manag*. 4(6), (2013) 631-638.

[27] C. Theivarasu, S. Mylsamy and N. Sivakumar. Cocoa Shell as adsorbent for the removal of methylene blue from aqueous solution: kinetic and equilibrium study. *Univ. J Env. Tech.*, 1 (2011) 70-78.

[28] T. Jia, Z. Xiaoyu, W. Xinhao and W. Lijuan. Removal of Malachite Green from Aqueous Solution Using Waste Newspaper Fiber. *Biores.* 7(3) (2012) 4307-4320.

[29] O.S. Bello, and M.A. Ahmad Preparation and characterization of activated carbon from rubber seed coat. *Bulg. J. Sci. Educ.*, 21(3) (2012) 236 – 345.

[30] O.S. Bello, T.A. Fatona, F.S. Falaye, O.M. Osuolale and V.O. Njoku Adsorption of eosin dye from aqueous solution using Groundnut Hull Based Activated Carbon: kinetic, Equilibrium, and thermodynamic studies. *Env. Eng. Sci.*, 29 (2011) 186 - 294.

[31] Amano Chocolate (2013). theobroma cacao – the Tree of Life: Climate. https://www.amanochocolate.com/blog/theobroma-cacao-the-tree-of-life-climate. (Accessed June 06, 2020). Amano Aritisan Chocolate, USA.

[32] Kew Science (2009). theobroma cacao (cocoa tree). https://www.kew.org/science-conservation/plants.fungi/theobroma-cacao-cocoa-tree. (Accessed June 06, 2020. The Royal Botanic Gardens, Kew, UK.

[33] Y.C. Uma, and S. Sharma. Removal of Malachite Green from Aqueous Solutions by Adsorption on to Timber Waste, *Int. J. Environ. Eng. Manag.*, 4(6) (2013) 631-638.

[34] B.C.S. Ferreira, F.S. Teodoro, A.B. Mageste, L.F. Gil, R.P. Freitas and L.V.A. Gurgel. Application of a new carboxylate functionalized sugarcane bagasse for adsorptive removal of crystal violet from aqueous solution: Kinetic, equilibrium and thermodynamic studies, *Industrial Crops and Products*, 65, (2015) 521–534.

[35] T.B. Pelosi, K.S.L. Lima and M.G.A. Viera. Acid orange 7 dye biosorption by *Salvinia natans* biomass. *Chem. Eng. Trans.*, 32 (2013) 1974-1981.

[36] T. Jia, Z. Xiaoyu, W. Xinhao and W. Lijuan. Removal of Malachite Green from Aqueous Solution Using Waste Newspaper Fiber, *Biores.*, 7(3) (2012) 4307-4320.

[37] S.A. Omotayo, O.O. Akeem, O.A. Abass, G.F. Abolaji and A.A. Segun. Adsorption of Methylene Blue from Aqueous Solution Using Steam-Activated Carbon Produced from *Lantana camara* Stem. . *J. Environ. Protect.*, 5 (2014) 1352-1363.

[38] N. El-Massaoudi, A. Lacherai, M. El-khomi, S. Bentaha and A. Dbik (2015). Modification of lignocellulosic biomass as agricultural waste for the biosorption of basic dye from aqueous solution. *J. Mater. Environ. Sci.*, 6(10) (2015) 2784-2794.

[39] J.R .Baseri, P.N. Palanisamy and P.S. Kuma. Adsorption of basic dyes from synthetic textile effluent by activated carbon prepared from *Thevetia peruviana*. *Indian J. Chem. Technol.*, 19 (2012) 311-314.

[40] R. Aravindhan, J.R. Rao and B.U. Nair. Removal of basic yellow dye from aqueous solution by sorption on green alga *Caulerpascal pelliformis. J. Hazard. Mater.*, 142, (2007) 68-76.

[41] K.V. Kumar, S. Sivanesan and N. Ramamurthi. Adsorption of malachite green onto *Pithophora* sp., a fresh water alga: Equilibrium and kinetic modelling. *Process Biochem.*, 40 (2005) 2865-2872.

[42] S. Zohre, S.G. Ataalah and A. Mehdi. Experimental study of methylene blue adsorption from aqueous solution onto carbon nano tubes. *International J. Water Res. Environ. Eng.* 2(2) (2009) 16-28.

[43] O. Amrhar, H. Nassali, and M.S. Elyoubi, Adsorption of a cationic dye, methylene blue onto Moroccan illitic clay. *J. Mater. Environ. Sci. 6*(11) (2015) 3054-3065.

[44] A.L. Prasad and T. Santhi. Adsorption of hazardous cationic dyes from aqueous solution onto Acacia nilotica leaves as an eco friendly adsorbent. *Sustain. Environ. Res.*, 22(2) (2012) 113-122.

[45] A.K. Mishra and V.K. Verma. Kinetic and Isothermal modelling of adsorption of dyes unto rice husk carbon. *Global J.*, 12 (2006) 190-196.

[46] E. Aysun, A. Kezban, T. Sema and K. Hikmet. Removal of Remazol Brilliant Blue R dye from aqueous solutions by adsorption onto immobilized Scenedasmus quadricauda: Equilibrium and kinetic modeling studies. *Desalination*, 249 (2009) 1308-1314.

[47] T. M. Elmorsi. Equilibrium isotherms and kinetic studies of removal of methylene blue dye by adsorption onto

miswak leaves as a natural adsorbent. *J. Environ. Prot.*, 2(6) (2011) 817–827.

[48] I. Langmuir. The constitution and fundamental properties of solids and liquids, *J. Americ. Soc.*, 38 (11) (1916) 2221 – 2295.

[49] H.M.F. Freundlich. Uberdie adsorption in losungen. *Zeitschrift fur physikalische chemie*. 57 (1906) 385-470.

[50] N. Ayawei, A.N. Ebelegi, and D. Wankasi. Review: Modelling and Interpretation of Adsorption Isotherms. *J. Chem.*, (2017) 1-11 https://doi.org/10.1155/2017/3039817

[51] H.K. Boparai, M. Joseph and D. M. O'Carroll. Kinetics and thermodynamics of cadmium ion removal by adsorption onto nano zerovalent iron particles. *J. Haz. Mat.*, 186(1) (2011) 458–465.

[52] M. Temkin Die gas adsorption und der nernstsche wärmesatz. *Acta Physicochim URSS*, 1 (1934) 36–52.

[53] H. Shahbeig, N. Bagheri, S. A. Ghorbanian, A. Hallajisani and S. Poorkarimi. A new adsorption isotherm model of aqueous solutions on granular activated carbon," *World J. Model. Sim.*, 9(4) (2013) 243–254.

[54] K. Vijayaraghavan, T.V.N. Padmesh, K. Palanivelu, and M. Velan. Biosorption of nickel(II) ions onto *Sargassum wightii*: application of two-parameter and three-parameter isotherm models," *J. Haz. Mat.*, 133(1) (2006) 304–308.

[55] M.M. Dubinin. The potential theory of adsorption of gases and vapors for adsorbents with energetically non-uniform surface. *Chem. Rev.*, 60 (1960) 235–266.

[56] O.C. Elebi, C. Uzum, T. Shahwan and H. N. Erten. A radiotracer study of the adsorption behaviour of aqueous Ba^{2+} ions on nanoparticles of zero-valent iron. *J. Haz. Mat.*, 148(3) (2007) 761–767,

[57] C. Theivarasu and S. Mylsamy. Removal of malachite green from aqueous solution by activated carbon developed from cocoa (*Theobroma Cacao*) shell—A kinetic and equilibrium studies," *E-J. Chem.*, 8(1) (2011) S363–S371,.

[58] R. H. Fowler and E. A. Guggenheim. Statistical Thermodynamics, Cambridge University Press, London, England, 1939.

[59] K.Y. Foo and B.H. Hameed. Insights into the modeling of adsorption isotherm systems. *Chem. Eng. J.*, 156(1) (2010) 2–10.

[60] S.K. Knaebel. Adsorbent selection. *Int. J. Trend Res. Dev.*, in: Adsorption Research, Dublin, Ohio. 43016, (2004).

[61] A.V.C. Kiseler. Vapour adsorption in the formation of adsorbate Mollecule Complexes on the surface. *Kolloid Zhur*., 20 (1958) 338–348.

[62] M. Gubernak, W. Zapała and K. Kaczmarski. Analysis of amylbenzene adsorption equilibria on an RP-18e chromatographic column. *Acta Chromatographica.*, 13(2003) 38–59.

[63] O. Hamdaoui and E. Naffrechoux. Modelling of adsorption isotherms of phenol and chlorophenols onto granular activated carbon. Part II. Models with more than two parameters. *J. Haz. Mat.*, 147(1) (2007) 401–411.

[64] A. Achmad, J. Kassim, T. K. Suan, R. C. Amat, and T. L. Seey. Equilibrium, kinetic and thermodynamic studies on the adsorption of direct dye onto a novel green adsorbent developed from Uncaria gambir extract. *J. Phys. Sci.*, 23(1) (2012) 1–13.

[65] M. Davoundinejad and S. A. Gharbanian. Modelling of adsorption isotherm of benzoic compounds onto GAC and introducing three new isotherm models using new concept of adsorption effective surface (AEC). *Academic J.*, 18(46) (2013) 2263–2275.

[66] O. Redlich and D.L. Peterson. A useful adsorption isotherm. *J. Phy. Chem.* 63 (6) (1959) 1024-1029

[67] F. Brouers and T. J. Al-Musawi. On the optimal use of isotherm models for the characterization of biosorption of lead onto algae. *J. Mol. Liq.*, (2015)212 46–51.

[68] C. Chen. Evaluation of equilibrium sorption isotherm equations. *Open Chem. Eng. J.*, 7(1) (2012) 24–44,

[69] R. Sips. On the structure of a catalyst surface. *J. Chem. Phys.*, 16 (1948) 490–500.

[70] S. Nethaji, A. Sivasamy and A. B. Mandal. Adsorption isotherms, kinetics and mechanism for the adsorption of cationic and anionic dyes onto carbonaceous particles prepared from *Juglans regia* shell biomass. *Int. J. Environ. Sci. Technol.*, 10 (2013) 231–242. http://doi.org/10.1007/s13762-012-0112-0

[71] M. F. Dilekoglu. Use of generic algorithm optimzation Techniques in the adsorption of phenol on Banana and grapefruit peels. *J. Chem. Soc. of Pak.*, 38(6) 2016.

[72] U. A. Edet and A. O. Ifelebuegu. Kinetics, Isotherms, and Thermodynamic Modeling of the Adsorption of Phosphates from Model Wastewater Using Recycled Brick Waste. *Processes*, 8(665) (2020)1-15; http://doi.org/10.3390/pr8060665

[73] S. Mustapha, D.T. Shuaib, M. M. Ndamitso, M. B. Etsuyankpa A. Sumaila U. M. Mohammed and M. B. Nasirudeen. Adsorption isotherm, kinetic and thermodynamic studies for the removal of Pb(II), Cd(II), Zn(II) and Cu(II) ions from aqueous solutions using *Albizia lebbeck* pods. *Applied Water Sci.*, 9(142) (2019) 1-12. https://doi.org/10.1007/s13201-019-1021-x

[74] Benhachem FZ, Attar T, Bouabdallah F. Kinetic study of adsorption methylene blue dye from aqueous solutions using activated carbon. Chem. Rev. Lett. 2019, 2(1), 33-39 http://doi.org/10.22034/CRL.2019.87964.

[75] K. L. Tan and B.H. Hameed. Insight into the adsorption kinetics models for the removal of contaminants from aqueous solutions. *J. Taiwan Institute of Chem. Eng.* 74 (2017) 25-48

[76] D.O. Omokpariola and J. N. Otuosorochi. Batch adsorption studies on Rice husk using methyl violet. *World News of Natural Sci.* 33 (2020) 48-63

[77] H.N. Tran, S.J. You, A. Hosseini-Bandegharaei, and H.P. Chao. Mistakes and inconsistencies regarding adsorption of contaminants from aqueous solutions: A critical review. *Water Res.*, 120 (2017) 88-116.

[78] E.S. Abechi, C.E. Gimba, A. Uzairu and J.A. Kagbu. Kinetics of adsorption of methylene blue onto activated carbon prepared from palm kernel shell. *Arch. Appl. Sci. Res.* 3 (2011) 154–164.

[79] W.H. Cheung, Y.S. Szeto, G. McKay. Intraparticle diffusion processes during acid dye adsorption onto chitosan. *Bioresour. Technol.* 98:(2007) 2897–2904

[80] W.J. Weber and J.C. Morris. Kinetics of adsorption on carbon from solution. *J Sanit Eng Div*., 89 (1963) 31-60.

[81] G.E. Boyd, J. Schubert and A.W. Adamson. The exchange adsorption of ions from aqueous solutions by organic zeolites. Ion-exchange equilibria. *J. Amer. Chem. Soc*. 69(11) (1947) 2818-2829

[82] H. Tang, W. Zhou and L. Zhang. Adsorption isotherms and kinetics studies of malachite green on chitin hydrogels. *J. Haz. Mat.*, 209–210 (2012) 218-225

[83] G.W. Kajjumba, S. Aydın and S. Güneysu. Adsorption isotherms and kinetics of vanadium by shale and coal waste. *Ads. Sci. & Technol.*, 36(3–4) (2018) 936-952.

[84] G.L. Dotto and L.A.A. Pinto. Adsorption of food dyes onto chitosan: Optimization process and kinetic. *Carbohydrate Polymers*. 2011;84(1):231-238.

[85] X. Yuan, W. Xia, J. An, J. Yin, X. Zhou and W. Yang. Kinetic and Thermodynamic Studies on the Phosphate Adsorption Removal by Dolomite Mineral. *J. Chem.* (2015) 1–8.

[86] R. Subha and C. Namasivayam. Modelling of Adsorption Isotherms and Kinetics of 2, 4, 6-Trichlorophenol Onto Microporous $ZnCl_2$ Activated Coir Pith Carbon. *J. Environ. Eng. Manag.* 18 (2008) 275–280.

[87] N. Ertugay and E. Malkoc. Adsorption Isotherm, Kinetic and Thermodynamic Studies for Methylene Blue from Aqueous Solution by Needles of *Pinus Sylvestris* L. *Pol. J. Environ. Stud.* 23(6) (2014) 1995-2006.

[88] D.O. Omokpariola and J. N. Otuosorochi. Adsorption of Congo red dye using Rice husk. *World Sci. News* 150 (2020) 22 – 38.

[89] A.O. Ifelebuegu, J.E. Ukpebor, C.C. Obidiegwu and B.C. Kwofi, Comparative potential of black tea leaves waste to granular activated carbon in adsorption of endocrine disrupting compounds from aqueous solution. *Glob. J. Environ. Sci. Manag.*, 1 (2015) 205–214.